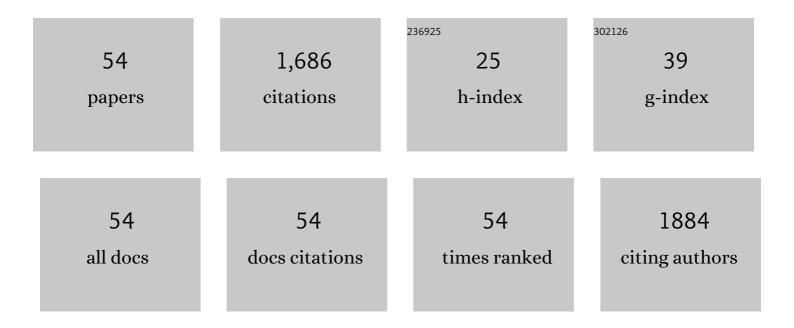
## Yan-Feng Dang

List of Publications by Year in descending order

Source: https://exaly.com/author-pdf/6844397/publications.pdf Version: 2024-02-01



YAN-FENC DANC

#	Article	IF	CITATIONS
1	Dispersion and Steric Effects on Enantio-/Diastereoselectivities in Synergistic Dual Transition-Metal Catalysis. Journal of the American Chemical Society, 2022, 144, 1971-1985.	13.7	80
2	Stereodivergent synthesis of enantioenriched azepino[3,4,5- <i>cd</i> ]-indoles <i>via</i> cooperative Cu/Ir-catalyzed asymmetric allylic alkylation and intramolecular Friedel–Crafts reaction. Chemical Science, 2022, 13, 4801-4812.	7.4	32
3	Ligand-promoted palladium-catalyzed β-methylene C–H arylation of primary aldehydes. Chemical Science, 2022, 13, 5938-5943.	7.4	8
4	Cocrystal Engineering: Toward Solutionâ€Processed Nearâ€Infrared 2D Organic Cocrystals for Broadband Photodetection. Angewandte Chemie - International Edition, 2021, 60, 6344-6350.	13.8	43
5	High-yield and sustainable synthesis of quinoidal compounds assisted by keto–enol tautomerism. Chemical Science, 2021, 12, 9366-9371.	7.4	10
6	Mechanism of Pd-catalysed C(sp <sup>3</sup> )–H arylation of thioethers with Ag( <scp>i</scp> ) additives. Organic and Biomolecular Chemistry, 2021, 19, 6766-6770.	2.8	3
7	Origins of ligand-controlled diastereoselectivity in dirhodium-catalysed direct amination of aliphatic C(sp <sup>3</sup> )–H bonds. Catalysis Science and Technology, 2021, 11, 6960-6964.	4.1	2
8	Mechanistic studies of Cp*Ir( <scp>iii</scp> )/Cp*Rh( <scp>iii</scp> )-catalyzed branch-selective allylic C–H amidation: why is Cp*Ir( <scp>iii</scp> ) superior to Cp*Rh( <scp>iii</scp> )?. Organic and Biomolecular Chemistry, 2021, 19, 3850-3858.	2.8	4
9	Cocrystal Engineering: Toward Solutionâ€Processed Nearâ€Infrared 2D Organic Cocrystals for Broadband Photodetection. Angewandte Chemie, 2021, 133, 6414-6420.	2.0	5
10	Exploring the pivotal role of silver(I) additives in palladium-catalyzed NH2-directed C(sp3)–H arylation reactions. Chinese Chemical Letters, 2021, 32, 3980-3983.	9.0	6
11	Unveiling the Hidden Ïfâ€Ðimerization of a Kinetically Protected Olympicenyl Radical. Chemistry - A European Journal, 2021, 27, 8203-8213.	3.3	22
12	Post-Transition State Bifurcation in Iron-Catalyzed Arene Aminations. ACS Catalysis, 2021, 11, 6816-6824.	11.2	11
13	Tandem catalysis in electrochemical CO2 reduction reaction. Nano Research, 2021, 14, 4471-4486.	10.4	105
14	Constructing ABA- and ABCBA-Type Multiblock Copolyesters with Structural Diversity by Organocatalytic Self-Switchable Copolymerization. Macromolecules, 2021, 54, 6171-6181.	4.8	30
15	Mechanistic Origins of Stereodivergence in Asymmetric Cascade Allylation and Cyclization Reactions Enabled by Synergistic Cu/Ir Catalysis. ACS Catalysis, 2021, 11, 9008-9021.	11.2	33
16	Mechanistic Studies of Copper(I)-Catalyzed Stereoselective [2,3]-Sigmatropic Rearrangements of Diazoesters with Allylic Iodides/Sulfides. ACS Catalysis, 2021, 11, 691-702.	11.2	16
17	Insights into the mechanism and regioselectivity in Ni-catalysed redox-relay migratory hydroarylation of alkenes with arylborons. Chemical Communications, 2021, 57, 13610-13613.	4.1	6
18	DFT Mechanistic Account for the Site Selectivity of Electron-Rich C(sp <sup>3</sup> )–H Bond in the Manganese-Catalyzed Aminations. Organic Letters, 2020, 22, 453-457.	4.6	25

YAN-FENG DANG

#	Article	IF	CITATIONS
19	Origins of Chemoselectivity in the Ni-Catalyzed Biaryl and Pd-Catalyzed Acyl Suzuki–Miyaura Cross-Coupling of <i>N</i> -Acetyl-Amides. Journal of Organic Chemistry, 2020, 85, 833-840.	3.2	12
20	Direct Arylation Polycondensation of Chlorinated Thiophene Derivatives to High-Mobility Conjugated Polymers. Macromolecules, 2020, 53, 10147-10154.	4.8	27
21	Mechanistic Studies of Nickel-Catalyzed Hydroarylation of Styrenes. Organic Letters, 2020, 22, 8998-9003.	4.6	22
22	Stable Olympicenyl Radicals and Their π-Dimers. Journal of the American Chemical Society, 2020, 142, 11022-11031.	13.7	63
23	Red-emissive poly(phenylene vinylene)-derivated semiconductors with well-balanced ambipolar electrical transporting properties. Journal of Materials Chemistry C, 2020, 8, 10868-10879.	5.5	18
24	Suzuki–Miyaura Cross-Coupling of Sulfoxides. ACS Catalysis, 2020, 10, 8168-8176.	11.2	29
25	High-mobility organic single-crystalline transistors with anisotropic transport based on high symmetrical "H―shaped heteroarene derivatives. Journal of Materials Chemistry C, 2020, 8, 11477-11484.	5.5	5
26	Origins of Unconventional γ Site Selectivity in Palladium-Catalyzed C(sp <sup>3</sup> )–H Activation and Arylation of Aliphatic Alcohols. Organic Letters, 2020, 22, 1464-1468.	4.6	18
27	A "Phase Separation―Molecular Design Strategy Towards Largeâ€Area 2D Molecular Crystals. Advanced Materials, 2019, 31, e1901437.	21.0	44
28	Organic Single Crystals: A "Phase Separation―Molecular Design Strategy Towards Largeâ€Area 2D Molecular Crystals (Adv. Mater. 35/2019). Advanced Materials, 2019, 31, 1970251.	21.0	2
29	Synthesis, catalysis, and DFT study of a ruthenium carbene complex bearing a 1,2-dicarbadodecaborane (12)-1,2-dithiolate ligand. Dalton Transactions, 2019, 48, 2646-2656.	3.3	4
30	Mesopolymer synthesis by ligand-modulated direct arylation polycondensation towards n-type and ambipolar conjugated systems. Nature Chemistry, 2019, 11, 271-277.	13.6	115
31	Unveiling the mechanism and regioselectivity of iron-dipyrrinato-catalyzed intramolecular C(sp <sup>3</sup> )–H amination of alkyl azides. Catalysis Science and Technology, 2019, 9, 1279-1288.	4.1	11
32	Smallâ€Moleculeâ€Doped Organic Crystals with Longâ€Persistent Luminescence. Advanced Functional Materials, 2019, 29, 1902503.	14.9	80
33	Solar Thermal Storage and Room-Temperature Fast Release Using a Uniform Flexible Azobenzene-Grafted Polynorborene Film Enhanced by Stretching. Macromolecules, 2019, 52, 4222-4231.	4.8	34
34	Mechanism of the Palladium-Catalyzed C(sp <sup>3</sup> )–H Arylation of Aliphatic Amines: Unraveling the Crucial Role of Silver(I) Additives. ACS Catalysis, 2019, 9, 6672-6680.	11.2	38
35	Sonogashira Cross-Coupling of Aryltrimethylammonium Salts. ACS Catalysis, 2019, 9, 3730-3736.	11.2	43
36	Ultratrace Naked-Eye Colorimetric Ratio Assay of Chromium(III) Ion in Aqueous Solution via Stimuli-Responsive Morphological Transformation of Silver Nanoflakes. Analytical Chemistry, 2019, 91, 4031-4038.	6.5	39

Yan-Feng Dang

#	Article	IF	CITATIONS
37	Mechanistic Study of Manganese-Catalyzed C–H Bond Functionalizations: Factors Controlling the Competition between Hydroarylation and Cyclization. Journal of Organic Chemistry, 2019, 84, 1916-1924.	3.2	11
38	Preparation of Thioanisole Biscarbanion and C–H Lithiation/Annulation Reactions for the Access of Five-Membered Heterocycles. Organic Letters, 2018, 20, 3161-3165.	4.6	12
39	Mechanistic understanding of [Rh(NHC)]-catalyzed intramolecular [5 + 2] cycloadditions of vinyloxiranes and vinylcyclopropanes with alkynes. Organic and Biomolecular Chemistry, 2018, 16, 4295-4303.	2.8	8
40	How Does Palladium–Amino Acid Cooperative Catalysis Enable Regio- and Stereoselective C(sp <sup>3</sup> )–H Functionalization in Aldehydes and Ketones? A DFT Mechanistic Study. ACS Catalysis, 2018, 8, 7698-7709.	11.2	38
41	A strategy for developing metal-free hydrogenation catalysts: a DFT proof-of-principle study. Dalton Transactions, 2018, 47, 7709-7714.	3.3	4
42	The Origins of the Differences between Alkyne Hydroalkoxylations Catalyzed by 8â€Quinolinolato―and Dipyrrinatoâ€Ligated Rh <sup>I</sup> Complexes: A DFT Mechanistic Study. European Journal of Inorganic Chemistry, 2017, 2017, 2713-2722.	2.0	7
43	Differences between the elimination of early and late transition metals: DFT mechanistic insights into the titanium-catalyzed synthesis of pyrroles from alkynes and diazenes. Chemical Science, 2017, 8, 2413-2425.	7.4	27
44	Formylation or methylation: what determines the chemoselectivity of the reaction of amine, CO <sub>2</sub> , and hydrosilane catalyzed by 1,3,2-diazaphospholene?. Chemical Science, 2017, 8, 7637-7650.	7.4	28
45	How Does an Earth-Abundant Copper-Based Catalyst Achieve Anti-Markovnikov Hydrobromination of Alkynes? A DFT Mechanistic Study. Organometallics, 2016, 35, 1923-1930.	2.3	16
46	Organocatalytic Enantioselective Decarboxylative Michael Addition of βâ€Keto Acids to Dicyanoolefins and Disulfonylolefins. Advanced Synthesis and Catalysis, 2016, 358, 2721-2726.	4.3	35
47	Unveiling Secrets of Overcoming the "Heteroatom Problem―in Palladium-Catalyzed Aerobic C–H Functionalization of Heterocycles: A DFT Mechanistic Study. Journal of the American Chemical Society, 2016, 138, 2712-2723.	13.7	65
48	The Mechanism of a Ligand-Promoted C(sp <sup>3</sup> )–H Activation and Arylation Reaction via Palladium Catalysis: Theoretical Demonstration of a Pd(II)/Pd(IV) Redox Manifold. Journal of the American Chemical Society, 2015, 137, 2006-2014.	13.7	106
49	Mechanistic Insight into Ketone α-Alkylation with Unactivated Olefins via C–H Activation Promoted by Metal–Organic Cooperative Catalysis (MOCC): Enriching the MOCC Chemistry. Journal of the American Chemical Society, 2015, 137, 6279-6291.	13.7	66
50	Depolymerization of Oxidized Lignin Catalyzed by Formic Acid Exploits an Unconventional Elimination Mechanism Involving 3c–4e Bonding: A DFT Mechanistic Study. ACS Catalysis, 2015, 5, 6386-6396.	11.2	46
51	Mechanism of <i>Z</i> -Selective Olefin Metathesis Catalyzed by a Ruthenium Monothiolate Carbene Complex: A DFT Study. Organometallics, 2014, 33, 4290-4294.	2.3	20
52	Mechanistic Origins of Chemo- and Regioselectivity of Ru(II)-Catalyzed Reactions Involving <i>ortho</i> -Alkenylarylacetylene, Alkyne, and Methanol: The Crucial Role of a Chameleon-like Intermediate. Journal of Organic Chemistry, 2014, 79, 9046-9064.	3.2	8
53	A Computational Mechanistic Study of an Unprecedented Heck-Type Relay Reaction: Insight into the Origins of Regio- and Enantioselectivities. Journal of the American Chemical Society, 2014, 136, 986-998.	13.7	118
54	Mechanism and Origins of <i>Z</i> Selectivity of the Catalytic Hydroalkoxylation of Alkynes via Rhodium Vinylidene Complexes To Produce Enol Ethers. Organometallics, 2013, 32, 2804-2813.	2.3	26